



1 **Climate simulations and pollen data reveal the distribution**
2 **and connectivity of temperate tree populations in eastern**
3 **Asia during the Last Glacial Maximum**

4 Suzanne Alice Ghislaine Leroy ^{1*}, Klaus Arpe ^{2*}, Uwe Mikolajewicz², and Jing Wu ³

5 1) Aix Marseille Univ, CNRS, Minist Culture, LAMPEA, UMR 7269, 5 rue du Château de l'Horloge, BP
6 647, 13094 Aix-en-Provence Cedex 2, France

7 2) Max-Planck-Institute for Meteorology, Hamburg, Germany, retired

8 3) Institute of Geology and Geophysics, Chinese Academy of Science (IGGCAS)

9 Beijing, 100029, P. R. China

10

11 * corresponding author

12 klaus.arpe@mpimet.mpg.de leroy@msh.univ-aix.fr,

13 **ABSTRACT**

14 Publications on temperate deciduous tree refugia in Europe are abundant, but little is known about
15 the patterns of temperate tree refugia in eastern Asia, an area where biodiversity survived
16 Quaternary glaciations and which has the world's most diverse temperate flora. Our goal is to
17 compare climate model simulations with pollen data in order to establish the location of glacial
18 refugia during the Last Glacial Maximum (LGM) period. Limits in which temperate deciduous
19 trees can survive are taken from the literature. The model outputs are first tested for the present by
20 comparing climate models with published modern pollen data. As this method turned out to be
21 satisfactory for the present, the same approach was used for the LGM, Climate model simulations
22 (ECHAM5 T106), statistically further down-scaled, are used to infer the temperate deciduous trees
23 distribution during the LGM. These were compared with available fossil temperate tree pollen
24 occurrences.

25



26 The impact of the LGM on the eastern Asia climate was much weaker than on the European
27 climate. The area of possible tree growth shifts only by about 2° to the south between the present
28 and the LGM. This contributes to explain the greater biodiversity of forests in eastern Asia
29 compared to Europe. Climate simulations and the available, although fractional, fossil pollen data
30 agree. Therefore climate estimations can safely be used to fill areas without pollen data by
31 mapping potential refugia distributions. The results show two important areas with population
32 connectivity: the Yellow Sea emerged shelf and the southern Himalayas. These two areas were
33 suitable for temperate deciduous tree growth, providing corridors for population migration and
34 connectivity (i.e. less population fragmentation) in glacial and in interglacial periods. Many tree
35 populations live in interglacial refugia; not glacial ones. The fact that the model simulation for the
36 LGM fits so well with observed pollen distribution is another indication that the used model is
37 good to simulate also the LGM period.

38 **Key words**

39 Eastern Asia, ECHAM5 model, Last Glacial Maximum, pollen, temperate deciduous trees,
40 population connectivity

41 **Supplementary information** is added, discussing relevant problems with analysis and model data

42 **Introduction** Eastern Asia temperate deciduous forests boast the world's most diverse temperate
43 deciduous forest flora (Donoghue and Smith, 2004; Qiu et al., 2011). They also contain the highest
44 numbers of Tertiary relict taxa that have disappeared from Europe (Milne and Abbott, 2002;
45 Svenning, 2003), such as *Carya* and *Parrotia* (Li and Del Tredici, 2008; Orain et al., 2013). The
46 reason for this situation should be sought in the history of these forests through Quaternary
47 glaciations and earlier. The last time when these forests had a considerable reduction of their
48 population or underwent a shift of their distribution was during the Last Glacial Maximum (LGM),
49 i.e. 21,000 years ago. On different continents, this happened in different ways due to the climate of
50 the area, the topography (including the orientation of the main mountain ranges that may act as



51 geographical corridors or barriers), the location and extent of icecaps and the extent of emerged
52 coastal shelves. In Europe, during the LGM, the temperate deciduous forests, especially the warm-
53 temperate tree species, died out in much of northern and central Europe and survived in refugia in
54 the mountainous areas of the three southern peninsulas: Iberia, Italy and the Balkans, as well as in
55 some smaller areas around the Black Sea and the southern Caspian Sea (Leroy and Arpe, 2007;
56 Arpe et al., 2011).

57 Various methods have been used to establish the locations of glacial refugia of temperate
58 deciduous trees during the LGM in Eastern Asia. For example, population distributions have been
59 published based on phylogenetic data in Eastern Asia (Qian and Ricklefs, 2000) and based on
60 biomisation using palaeo-data for the Japanese archipelago (Takahara et al., 2000; Gotanda and
61 Yasuda, 2008) and for China (Harrison et al., 2001). A disagreement regarding the location of
62 temperate tree refugia in China, especially at its northern limit, has appeared: Harrison et al. (2001)
63 proposed the northern limit of the temperate deciduous forest biome to have retreated far south
64 (south of 35° N) versus Qian and Ricklefs (2000) who suggested an extension of the temperate
65 forest over the emerged continental shelf. Qian and Ricklefs (2000) highlighted the important role
66 played by physiography heterogeneity, climatic change and sea-level changes in allopatric
67 speciation. According to the results of their ecological analysis, a temperate tree population
68 extended across the emerged shelf and linked populations in China, Korea and Japan during glacial
69 times. This led to the concept of interglacial fragmentation and refugia.

70 Additional information from phylogenetics of temperate deciduous trees should also be considered
71 for phylogeography purposes. But few trees/bushes belonging to the deciduous forest have been
72 analysed so far. A temperate deciduous bush, *Ostryopsis davidiana*, indicates multiple LGM
73 refugia both south and north of the Qin Mountains (Tian et al., 2009).

74 To be complete, it should be mentioned that the distribution of key temperate tree biomes (discrete
75 points) for the LGM can be found in Ni et al. (2014).



76 Our aim is to contribute to this debate on the northern limit of temperate deciduous trees by using
77 another approach to ecology, to biomisation and to phylogeography: i.e one based on climate
78 model simulations. The results from this approach are validated by pollen data, whose amount has
79 increased spectacularly since 2010. Distribution maps are then produced.

80 **2 MATERIAL AND METHODS**

81 The climatic data, model and methods used in this study are described by Leroy and Arpe (2007)
82 and Arpe *et al.* (2011) in more detail. Coupled ECHAM5-MPIOM atmosphere ocean model
83 simulations were carried out, though with a very low horizontal resolution of T31. In such a
84 coupled model, the atmosphere as well as the ocean and the vegetation were simulated and interact
85 with each other and generated their own Sea Surface Temperature (SST) and vegetation
86 parameters. These SSTs and vegetation parameters were then used for uncoupled ECHAM5 T106
87 atmospheric simulations. The ECHAM models including the coupled ocean model were developed
88 at the Max-Planck Institute for Meteorology in Hamburg (MPI).

89 The models were run on one hand with the present-day conditions concerning the orography, solar
90 radiation, ice cover and CO₂ and on the other hand under LGM conditions concerning the same
91 parameters (e.g. atmospheric CO₂ concentration at 185 ppm). The simulations for the present and
92 the LGM with a T106 resolution (approx. 1.125° horizontal resolution) model with 39 atmospheric
93 vertical levels were carried out with the ECHAM5 atmospheric model (Roeckner *et al.*, 2003). The
94 boundary data, e.g. the SST and vegetation parameters, were taken from the coupled ECHAM5-
95 MPIOM atmosphere ocean dynamic vegetation model (Mikolajewicz *et al.*, 2007) simulations,
96 which have been made for the present and the LGM with a spectral resolution of T31
97 (corresponding to approx. 3.75°) and 19 vertical levels. The experimental setup is largely
98 consistent with the Paleoclimate Modelling Intercomparison Project phase 2 PMIP2 (Braconnot *et*
99 *al.*, 2007). These SSTs were corrected for systematic errors of the coupled run by adding the SST
100 differences between observed SSTs and simulated ones for the present, the corrections are
101 generally below 3°C.



102 In Arpe et al. (2011), comparisons of the model generated SSTs with other reconstructions, e.g.
103 from the MARGO project (Kucera et al., 2005), were performed and good agreement was found.
104 Differences to the CLIMAP (1981) reconstruction agree with findings by PMIP2 (Braconnot et al.,
105 2007). Also other information from the LGM gave further confidence in the performance of the
106 model. In Arpe et al. (2011), the importance of a high resolution is stressed. Therefore, we use here
107 again the T106 model. Intuitively one assumes that the model that provides good estimations for
108 the present climate would also be best for simulating a climate with a different external forcing
109 such as during the LGM. Indeed Arpe et al. (2011) found good correspondence between pollen
110 findings for the LGM and the estimation of possible tree growth for Europe, which increased
111 confidence in that model. As the climate of Eastern Asia is quite different to that of Europe, we try
112 to find further evidence for the high performance of the model in Eastern Asia.

113 It is generally assumed that results from model simulations become more robust when using an
114 ensemble of different model simulations; but we did not do that. As the ECHAM models have been
115 shown by Reichler and Kim (2008) to belong to the best ones and by including other ones, we
116 would only dilute our results. Further, most of the available simulations are of much lower
117 resolution than T106, that used here, and which we believe is essential for a region of diverse
118 topography such as Eastern Asia. When combining the results of different models, an interpolation
119 to a common grid is inevitable and that creates some smoothing with a further loss of resolution.

120 Nevertheless, even a T106 model resolution might not be sufficient for our investigation. Kim et al.
121 (2008) demonstrate the importance of a high resolution with their model, among others, for the
122 response of the Eastern Asian summer monsoon under LGM conditions. Therefore, we did a down-
123 scaling to a 0.5° resolution. For that, the differences between the model simulations for the LGM
124 and the present are added to a high-resolution present-day climatology. The climatology that
125 seemed best for our investigation is that of Cramer and Leemans (Leemans, R. and Cramer (1991) ;
126 Cramer, 1996), below abbreviated as “C&L”. With this method, the impact of possible systematic
127 errors of the model is reduced. This method works only if the simulations are already reasonable;



128 otherwise it might happen that e.g. negative precipitation amounts may occur. We could use this
129 method only for the precipitation and 2m air temperature (T2m) while the winds had to be taken
130 directly from the model simulations.

131 To improve the understanding of limitations in the climate data, estimates of the present
132 climatology with data from the Global Precipitation Climate Center (GPCC) (Schneider et al.,
133 2011; Becker et al., 2013; GPCC, 2013) and with data from the ECMWF interim reanalyses (ERA)
134 (Dee et al., 2011; ECMWF, 2014) are used.

135 Lower CO₂ concentration in the atmosphere during the LGM has caused a decline of pollen
136 production. Therefore low pollen concentrations or influxes may already be indicative of the
137 presence of trees (Ziska and Caulfield, 2000; Leroy, 2007). It should be noted that we are here not
138 working at the level of forests, nor of biomes. Hence it is considered that pollen sites will reliably
139 indicate the survival of temperate deciduous trees (summer-green and broadleaf) if records have a
140 sub-continuous curve of at least one temperate taxon such as deciduous *Quercus*, *Ulmus*, *Carpinus*
141 or *Tilia*. The study focuses on the period of the LGM, hence on an age of 21 ± 2 cal ka BP (Mix et
142 al., 2001). The geographical areas of China, Japan, SE Russia, Korea and the Himalayas are
143 explored. The dataset includes terrestrial and marine sites. A literature review of pollen data was
144 made. It was first based on the large compilations of Cao et al. (2013) mainly for China and of
145 Gotanda and Yasuda (2008) for Japan. Then this was enlarged geographically and with an update
146 including more recent publications.

147 Modern pollen assemblages were used to check the validity of the tree growth limits chosen. The
148 following databases were used: Zheng et al. (2014) for China and Gotanda et al. (2002) for Japan.
149 This was complemented by local studies such as by Park (2011) and Park and Park (2015) for
150 Korea and the Himalayas (Fuji and Sakai, 2002; Chung et al., 2010; Kotlia et al., 2010; Yi and
151 Kim, 2010). It was not aimed to be exhaustive. From these databases, the occurrences of temperate
152 deciduous trees (deciduous *Quercus*, *Ulmus*, *Tilia*, *Carpinus*, and others) of at least 0.5% were
153 selected.

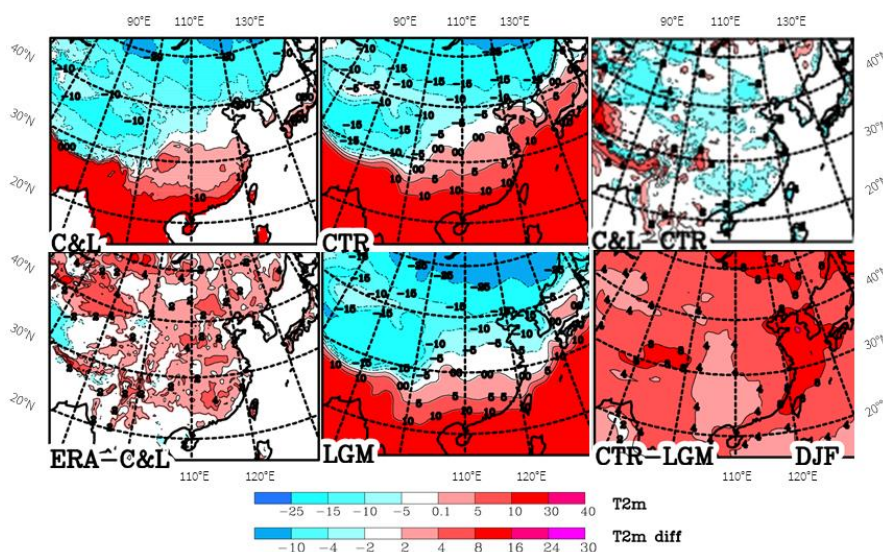


154 **3 CLIMATE OF EASTERN ASIA**

155 In our earlier investigations on glacial refugia of trees over Europe (Leroy and Arpe 2007; Arpe et
156 al., 2011), limiting factors for possible tree growth were the precipitation during summer, the mean
157 temperature of the coldest months and the growing degree days ($>5^{\circ}\text{C}$) (GDD5), the latter is
158 related to the summer temperatures. The climate of Eastern Asia is different to that of Europe and a
159 short review of its climate is therefore needed in order to adapt the limits.

160 The climate of Eastern Asia is dominated by the monsoon (more information in Appendix S1 of
161 Supporting Information) as well as by its very strong topographic variability. The latter makes it
162 difficult to create a reliable climatology on a regular grid. This is demonstrated for air temperature
163 T2m) during December to February (DJF) by comparing the C&L climatology with a long-term
164 mean from the ECMWF interim reanalysis (Dee et al. 2011; ECMWF-ERA. 2019) (ERA), CTR
165 and LGM simulations (Fig. 1).

166



167

168 Fig. 1: Climatological mean distribution of T2m over Eastern Asia for December to February
169 (DJF)

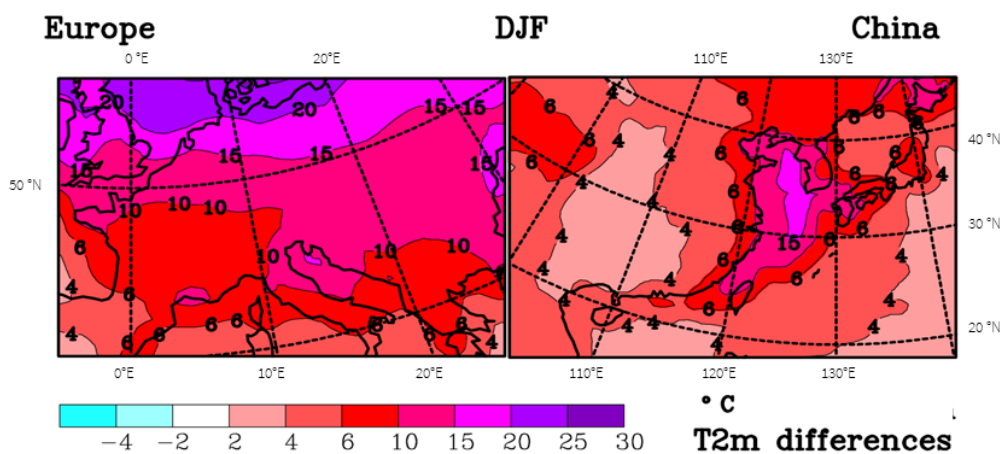
170 Values by Leemans, R. and Cramer (1991) (C&L), the ECMWF reanalysis (ERA) and model
171 simulations (CTR and LGM), as well as some differences between them.

172 Much stronger structures in the C&L climatology compared to the other climatologies can be seen
173 (Fig. 1). Moreover substantial differences are observed, e.g. the white band (-5 to 0°C) is
174 positioned about 5° further north in eastern Asia in ERA compared to C&L (not shown) with up to
175 4 °C warmer temperatures over a large part of Eastern Asia (panel ERA- C&L). For the Caspian
176 region, Molavi-Arabshahi et al. (2015) showed how biases of several °C in ERA can occur in
177 mountainous areas when the topographic height in the ECMWF model and the real topography are
178 different. So it is assumed that the warmer temperatures in ERA compared to C&L are due to this
179 analysis system. The climate simulation for the present (Fig. 1, CTR) agrees similarly well with
180 ERA and C&L, a little warmer than C&L and cooler than ERA (not shown).

181 A main purpose of different simulation periods (Fig. 1) is the display of changes from the LGM to
182 the present (Fig. 1 lower right). Over the Yellow Sea, temperatures differ by up to 16 °C, as a large



183 area of the ocean shelf emerged during the LGM, while the differences are much smaller for
184 continental China, mainly 4 to 5 °C. These changes between the present and the LGM are overall
185 much weaker than for Europe in winter (Fig. 2). Typical differences for continental central Europe
186 are 8-15 °C while they are only around 4-5 °C for the Eastern Asian continent. One has to take into
187 account that China is further south than central Europe, the central latitudes in the European map
188 are 45 to 50 °N while for China they are 32 to 37 °N, which contributes to explain the large
189 differences in the temperature change. Also the proximity of the Fennoscandian ice sheet is of
190 importance for the colder temperatures in Europe, as well the weakening of the Gulfstream, which
191 presently supplies Europe with warmer temperature. The strong temperature change over the
192 Yellow Sea is a consequence of the larger heat capacity of the ocean, which limits the winter-time
193 cooling under present-day conditions. At the LGM, this area was emerged due to the lower sea
194 level, which leads to much stronger winter-time cooling.
195
196

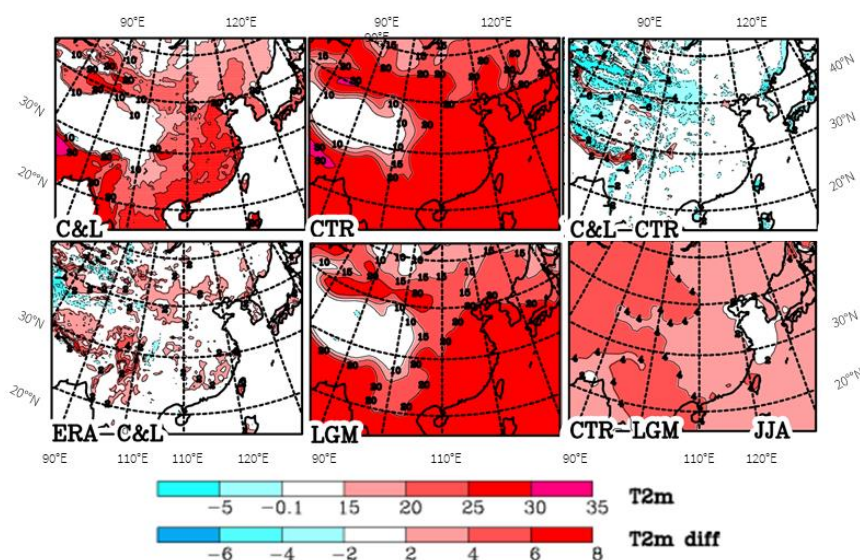


197
198 Fig. 2: Difference maps between simulated CTR and LGM T2m during winter (DJF) for Europe
199 and Eastern Asia.
200



201 The summer temperatures are shown in Fig. 3. ERA temperatures are often warmer by around 2 °C
202 than the ones in the C&L climatology (not shown). The differences between the present and the
203 LGM in the simulations increase from China's east coast of 2-3 °C to up to 6 °C over Tibet. This is
204 similar to what Tian and Jiang (2016) found in PMIP3 simulations; they state that the temperature
205 drop in the LGM is too low compared to proxy data. The summer temperatures are being used to
206 calculate the GDD5. For the small changes shown here, we do not expect that GDD5 does impose
207 much more limitation for the LGM than for the present for tree growth.

208



209

210 Fig. 3: Climatological mean distribution of temperature T2m over Eastern Asia for June, July
211 August (JJA)

212 Values by Leemans, R. and Cramer (1991) (C&L), the ECMWF reanalysis (ERA) and model
213 simulations (CTR and LGM), as well as some differences between them.

214



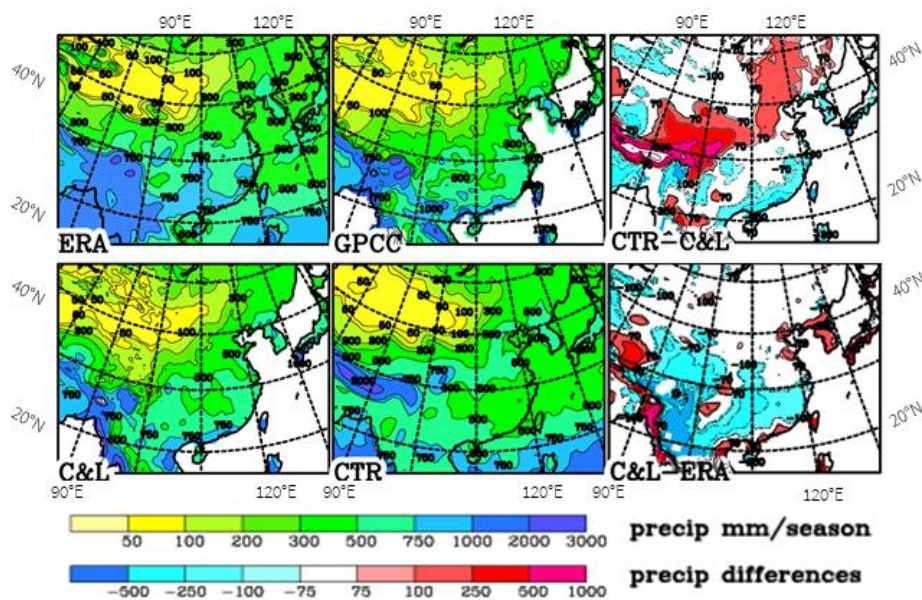
215 The difference maps for CTR-LGM temperatures show values over the ocean (Figs. 1 to 3).
216 These differences may have an important impact on continental temperatures. Therefore, it is
217 interesting to compare these data with other estimates of the SST. For example, Annan and
218 Hargreaves (2013) show annual means of SST differences of around 2°C for the South China
219 Sea while our simulations have slightly larger values of 2.5 to 3°C, though this falls within the
220 uncertainty range given by Annan and Hargreaves (2013). A main difference is less cooling
221 during the LGM in our estimates at the Gulf and Kuroshio currents off the USA or Japan coast
222 (not shown).

223 Summer precipitation is an important limiting factor for possible tree growth (Fig. 4). The sharp
224 gradient of precipitation along the southern slopes of the Himalayas in the three sets of analyses (the
225 climatology by C & L and the long-term means from ERA and GPCC) is clearly marked. The general
226 patterns agree in the three sets, though with some biases. C&L and GPCC agree best, probably;
227 because they are both based on precipitation observations at gauges. On the contrary, ERA is a model
228 product forced by a very large range and more evenly distributed observations; moreover ERA does
229 not use observed gauge precipitation. Differences between C&L and GPCC are mostly below 50
230 mm, especially in the northern areas where the precipitation is moderate. The differences between
231 C&L and ERA are also small in northern areas; but can become quite large where the amounts of
232 precipitation are large, mostly with ERA having larger precipitation amounts. The lower
233 precipitation rates in ERA for Korea and southern Japan in contrast to C&L and GPCC are
234 remarkable. Here the latter data are probably more accurate because this area is well-covered by
235 observations (Fig. S2.3) and the ERA model may not be able to resolve the strong topographic
236 structures. Many of the large uncertainties are probably due to the strong topographic structures over
237 Eastern Asia, which makes an analysis difficult and which is enhanced by a low density of
238 observational sites over western China (more information on precipitation accuracy in Appendix S2
239 of Supporting Information).

240 The systematic error of the model concerning China consists of the monsoon front being too far north
241 by 2° of latitude (Fig. S1.2) and with a too early northward propagation in the season (Appendix S1
11



242 of Supporting Information). As we only use the differences between the present and LGM this
243 systematic error is assumed to have only a minor impact on our results. As for Tian and Jiang (2016),
244 a general weakening of the monsoon is found for March to May. However in our simulation, it is
245 more a strengthening north of 32°N for May to August for precipitation and 80hPa wind. This
246 systematic error is assumed to have only a minor impact on our results. Indeed, most of the
247 differences turn out to be less important for the further use in this study, except larger precipitation
248 over western China at 37°N on the northern slope of the Kunlun Shan in the C&L data set, which is
249 investigated in more detail in Appendix S2 of Supporting Information.



250

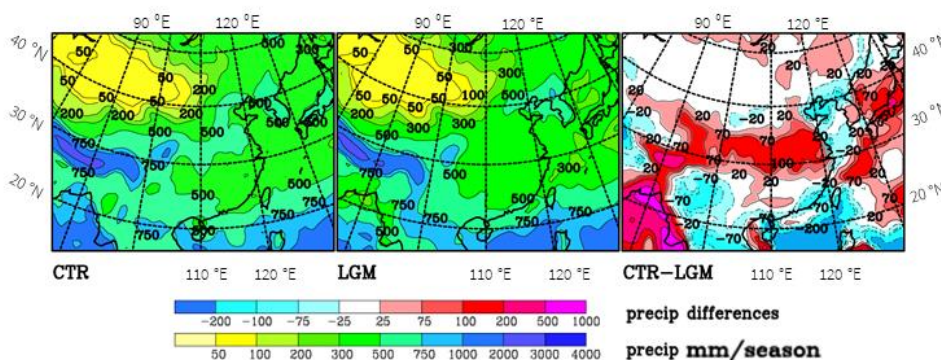
251 Fig. 4: Summer (JJA) precipitation over Eastern Asia as analyzed by Leemans, R. and Cramer
252 (1991) (C&L), ERA and GPCC and as simulated for the present (CTR). Differences between the
253 various fields are shown. Units: mm/season

254

255 Below we will concentrate on summer precipitation because that is the time when plants need water
256 most. Other scientists use the annual mean precipitation as a limiting factor (e.g. Tian et al., 2016).
257 When comparing the analyses with the model simulations for the present (CTR), one finds that the



258 model fits better to GPCC and least to ERA (Fig. 4). away from the high mountain ranges where the
259 agreements between the different precipitation climatologies is very low. The amounts of
260 precipitation in ERA is on a large scale higher than the other ones. For most of China south of 35°N
261 the precipitation in ERA is much lower than in the other climatologies.. The belt with stronger
262 precipitation at 25 to 35°N in CTR is assigned in Appendix S1 of Supporting Information to an
263 earlier northward propagation of the monsoon front in CTR compared to ERA, weakens from the
264 CTR to LGM, which results in a belt of largest differences between the present and the LGM of up
265 to 150 mm (Fig. 5). Kim et al. (2008) found similar differences in their higher resolution simulation,
266 though spreading further north. In Appendix S1 of Supporting Information, it is shown that the
267 monsoon, as represented by the wind direction, does not change much over the continent between
268 the present and the LGM, and with the monsoon front propagating northward already in June the
269 wind speeds increase. This is somewhat in contrast to results by Jiang and Lang (2010) who showed
270 for the ensemble mean of model simulations (all with a much lower horizontal resolution than the
271 one used here) a reduction of the JJA wind speeds. The lower JJA precipitation during LGM may
272 also result from lower temperatures during LGM, when the atmosphere can carry only a lower
273 amount of water vapour.
274 While Tian and Jiang (2016) found in PMIP3 simulations a general decrease of precipitation, we
275 find it only for a belt at 29-36° N where the model shows already a deficit for the present (CTR).



276



277 Fig. 5: Summer (JJA) precipitation simulated for and differences. Between CTR and LGM.

278 Units: mm/season.

279

280 4 COMPARING POLLEN INFORMATION WITH CLIMATIC DATA

281 In Leroy and Arpe (2007) and Arpe et al. (2011), climatic data were combined to find the areas
282 where temperate deciduous trees could survive due to limiting criteria and then compared that with
283 palaeo-data of such trees for Europe. The same method is now applied for Eastern. Europe is
284 limited to the south by steppe and by the Mediterranean Sea. However in E. Asia, a vast
285 subtropical area with deciduous temperate trees mixed with conifers and broadleaved evergreens
286 (i.e. between biomes TEDE and WTEM of Ni et al., 2010) lies south of the temperate deciduous
287 forest (Qiu et al., 2011). It was therefore essential to add a climatic limit to separate these two main
288 vegetation types In addition to the limits used for Europe, we add also a maximal winter
289 temperature (Tmax) which the climatological temperature must fall below to allow deciduous tree
290 will grow, suggested by Sitch et al. (2003) and Roche et al. (2007) (Table 1).Sitch et al. (2003)
291 require a less strong limit of -17 °C minimum temperature and +15.5 °C maximum temperature of
292 coldest month for temperate deciduous trees but only for very few sites such a relaxation of limits
293 would decrease the number of sites that fail the comparison with the climatological estimate.
294 Roche et al. (2007) used for temperate broadleaf forest Tmin=-2 °C and Tmax of +5 °C. We regard
295 a Tmin limit of -2 °C only valid for warm-loving deciduous trees.

296 Table 1: Limiting factors for temperate deciduous tree growth used in this study.

297 Tmin = minimum temperature of the coldest month, Tmax = maximum temperature of the coldest month,

298 GDD5 = growing degree days for which the excess over 5°C is accumulated for each day,

299 JJA precipitation =accumulated summer precipitation.

300

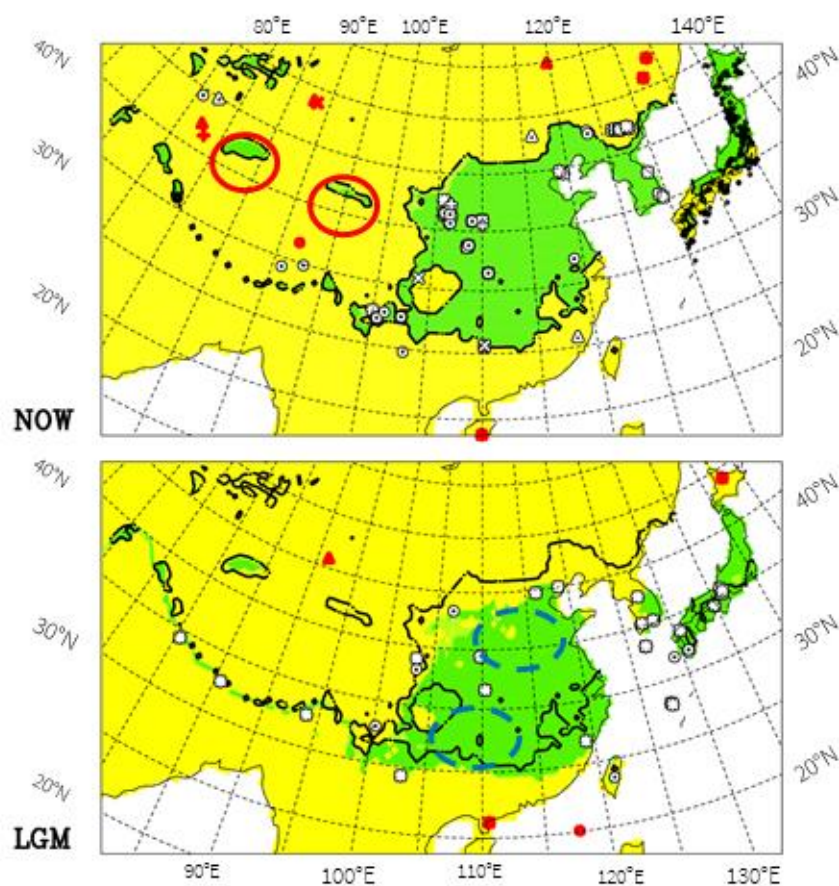
Tmin	Tmax in winter	GDD5	JJA precipitation
-15°C	+5°C	800	50 mm/summer



301

302

303 When combining these limits with the climate data we arrive at the distribution shown in Fig. 6.



304

305 FIG. 6

306

307 Fig. 6: Possible tree growth according to our limitations given in Table 1. Darker colours mean that
308 the climate data suggest possible tree growth. For easier comparison between the present (upper
309 panel) and the LGM (lower panel), the limits for the present are copied as a solid line into the



310 LGM panel. Markers indicate where and which tree pollen of deciduous trees are found. Markers:
311 circles = *Quercus*, squares = *Tilia*, triangles = *Ulmus*, plus = *Juglans* and stars = more than one
312 taxon. For modern-day sites in Japan only dots are used for clarity of the plot. Open markers = at
313 least within a distance of ± 3 grid points (~ 150 km radius) the climate data suggest possible tree
314 growth; otherwise filled markers. Red and blue (dashed) ovals show areas of interest mentioned in
315 the text.

316

317 Only very few stations with observed pollen are outside (not within a distance of ± 3 grid points,
318 i.e. about ~ 150 km radius) the area of possible tree growth according to our criteria (filled
319 markers). For the present, 13 out of 380 stations with observed deciduous tree pollen do not fit to
320 the climate data of the present, most of them because of too cold winter temperatures (-20 to -23
321 $^{\circ}\text{C}$), one at 91°E , 31°N because of a too short summer ($\text{GDD5} < 600$), two (both at 109°E , 18°N)
322 because of too warm winter temperatures ($>17^{\circ}\text{C}$) and one (77°E , 37°N) because of lack of
323 summer precipitation and too cold winter temperatures, though these are both near given limits.
324 South-eastern Japan is often too warm in winter for deciduous trees though there are many
325 observations in that area. These stations are, however, within 3 grid points to areas that are marked
326 as suitable for their growth.

327 In Fig. 6 for the present, two areas marked by red ovals in western China at latitude 37°N indicate
328 possible tree growth according to the climatic data where the precipitation in the C&L climatology
329 (Fig. 4) exceeds the ones of ERA and GPCC considerably. Also ERA and GPCC show relative
330 maxima at 37°N in that area but shifted by 5° to the east. We believe that the precipitation by
331 C&L is deficient here, as explained in Appendix S2 of Supporting Information. In the southern
332 China Sea around 120°E , 28°N only one marker with observed tree pollen for the LGM is shown in
333 fig. 6 although around that position four cores are available (see Table 2 for details). All four
334 observations agree with the possibility of trees according to the climate estimate. Because of the
335 use of marine sediment, pollen must have been transported from the land, which is further
336 discussed in the next section.



337 In Eastern Asia, some species might have evolved which are hardier than those of the same genus
338 present in Europe. Fang et al. (2009) show *Ulmus pumila* over large areas of northern China and
339 SE Siberia, a species that can withstand extremely cold temperatures in winter and drought (Solla
340 et al., 2005). *Ulmus* has the most failures in our comparison with model data. Fang et al. (2009)
341 show a wide spread of *Tilia amurensis* in NE China, SE Siberia and N Korea, which is also absent
342 from Europe. This tree, like the elm, is extremely frost hardy (Piggott, 2012).

343

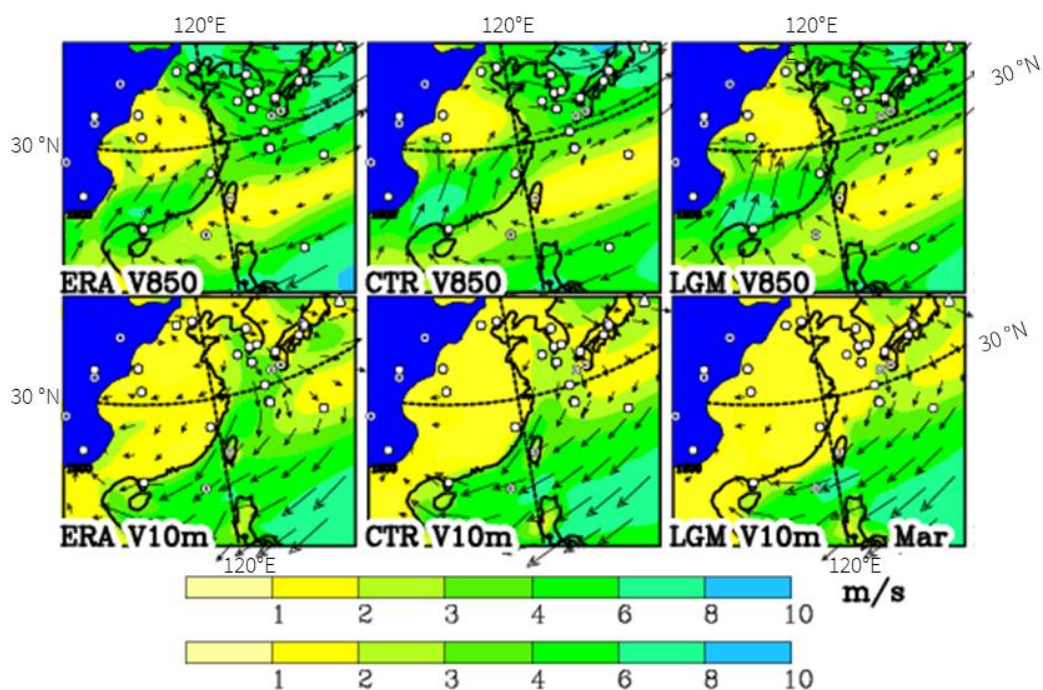
344 **5 POSSIBLE TREE GROWTH DURING THE LGM**

345 Thirty-five pollen sites for the LGM were used (Table 2). A good overall fit occurs between the
346 climate data and the LGM pollen data. In Fig. 6 lower panel, only two filled markers, not agreeing
347 with climate data, are found on the continent. The site of Huguangyan in the south has winter
348 temperatures higher than 10° C, which are too high for deciduous trees. In the north-west China in
349 the Tarim basin is another filled marker. The observation consists of only 1% pollen for *Ulmus*.
350 There the winter temperatures are -17 °C, just outside the limit used here (Table 1) but within the
351 limits suggested by Sitch et al. (2003). On Hokaido a filled marker indicates a disagreement between
352 climate and pollen observation but it is only slightly too cold in winter (-15.7 °C).

353 Four cores in the deep ocean in the S. China Sea are marked in Table 2 and Fig. 6 as not agreeing
354 with our given limits when using the down-scaled climate data, but because of the deep sea the pollen
355 must have been transported there. From Fig. 7, it can be concluded that the pollen could only have
356 come with the north-easterly 10m wind from Taiwan where also *Quercus* was found during the LGM
357 (Table 2). As the present blooming period for *Quercus variabilis*, a widespread species of the
358 deciduous forest, is January to March in Taiwan (Liao, 1996), the winds during March are shown in
359 Fig. 7, assuming a little later blooming period during the cooler LGM than presently, though the
360 wind fields for March and February are hardly different. When taking the wind at a higher level (850
361 hPa or around 1500m), the wind is blowing more from the east in accordance with the Ekman spiral
362 in the atmospheric boundary layer. Therefore pollen must have travelled near the surface when



363 coming from Taiwan or if it arrived at higher levels it may have come from the Philippines (Luzon)
364 that however seems to be too far south for deciduous oak and, moreover, this area is not suggested
365 in our estimate of having possible deciduous tree growth (Fig. 6).
366 Thus the area boundaries for the present and for the LGM are only slightly different with a shift for
367 the LGM by 2 to 3° to the south of both the northern and southern limits, and an eastwards shift of
368 the western boundary. In northern China, Korea and north Japan (Hokkaido), differences result
369 mainly from the winter minimum temperatures, as can be seen from Fig. 1 in which winter
370 temperatures drop by more than 6°C from the present to the LGM.



371
372 Fig. 7: 10m and 850hPa winds for March as analysed (ERA) and simulated for the present (CTR)
373 and LGM. Areas with topography above the 850hPa level are erased. Observational sites during
374 the LGM are indicated by markers
375



376 Table 2: Selected sites with observed pollen during the LGM. "*Quercus*" include deciduous
 377 *Quercus* and *Lepidobalanus*, "*Ulmus*" includes *Ulmus-Zelkova*, and "others" include: *Carya*, *Tilia*,
 378 *Carpinus*.
 379 "Agree" means that the observations agree with our estimates of possible tree growth as shown in
 380 Fig. 6 or 8 respectively.

381

382 Table 2a: east of 120°E

Lon E	Lat N	Site	Region	Alt/ depth in m	<i>Quercus</i>	<i>Ulmus</i>	Other	Agree	Author
126°32'	33°14'	HN-1, Hanon maar	Jeju Island	53			Y	Y	4
126°33'	33°15'	BH-4B	Jeju Island	53	Y	Y	Y	Y	5
126°52'	35°12'	Yeonjaedong Trench	Gwangju	20?	Y	Y		Y	6
127°13'	33°15'	UD-2	Hanam	19	Y	Y		Y	7
128°04'	35°10'	Pyonggeodong	Jinju	30			Y	Y	8
128°57'	38°33'	MD982195	N of E. China Sea	-746	Y			Y	9
130°23'	31°49'	Imutaik Pond	Southern Kyushu	330	Y			Y	10
130°23'	33°36'	Tenjin	Tenjin Fukuoka city, N Kyushu	0		Y	Y	Y	11
134°36'	34°24'	Ohnuma	Chugoku Mts	610	Y		Y	Y	12
135°48'	35°12'	Hatchodaira	Kyoto	810	Y	Y	Y	Y	13
135°53'	35°32'	Iwaya	Fukui	20		Y	Y	Y	14
135°53'	35°33'	Lake Mikata	C Japan	0		Y	Y	Y	15
138° 53'	36°49 '	Lake Nojiri	C Japan	250	Y	Y	Y	Y	16
140° 10'	36°03 '	Hanamuro River HS1	C Japan	5	Y	Y	Y	Y	17
139° 40'	36°41 '	Nakazato	C Japan	183	Y	Y	Y	Y	18
141° 47'	36°04 '	MD01-2421	off Kashima	- 2224	Y	Y	Y	Y	21c
130° 42'	35°56 '	KCES-1	Sea of Japan	- 1464	Y	Y		Y	19
142 12.08	41 10.64	C9001C	NE Japan	- 1180	Y	Y	Y	?	20
136°03	35°15'	BIW 95-4	Lake Biwa	85	Y	Y		Y	21a
142°28'	44°03 '	Kenbuchi	Hokaido	137	Y	Y	Y	N	21b

383



384 Authors: 4 Park and Park 2015; 5 Chung 2007; 6 Chung et al. 2010; 7 Yi and Kim 2010; 8 Chung et al. 2006; 9 Kawahata and
 385 Ohshima 2004; 10 Shimada et al. 2014; 11 Kuroda and Ota, 1978; 12 Miyoshi and Yano, 1986; 13 Takahara and Takeoka,
 386 1986; 14 Takahara and Takeoka, 1992; 15 Nakagawa et al. 2002; 16 Kumon et al. 2003; 17 Momohara et al. 2016; 18
 387 Nishiuchi et al. 2017; 19 Chen et al. 2016; 20 Sugaya et al. 2016; 21a Hayashi et al. 2010; 21b Igarachi and Zarov 2011; 21c
 388 Igarachi 2009
 389

390 Table 2b: west of 120°E

Lon E	Lat N	Site	Region	Alt/ depth in m	<i>Quercus</i>	<i>Ulmus</i>	Other	Agree	Author
80°08'	29°20'	Phulara palaeolake	Kumaun Himalaya	1500?	Y	Y	Y	Y	1
85°18'	27°14'	JW-3	Kathmandu valley	1300	Y		Y	Y	2
93°49'	27°32'	Ziro valley	Arunachal Pradesh	1570	Y		Y	Y	3
91°03'	40°47'	CK2	Tarim basin	780	Y			N	22
99°57'	27°55'	06SD, lake Shudu	Yunnan	3630	Y			N	23
102°47'	24°20'	XY08A, Xingyun Lake	C Yunnan	1772	Y		Y	Y	24
102°57'	33°57'	RM Ruergai	Zoige basin	3400	Y	Y		Y	26
103°30'	32°55'	Wasong	NE Tibetan Plateau	3490	Y			Y	27
106°30'	38°17'	Shuidonggou locality 2	Yinchuan, Ningxia	1200	Y	Y		Y	28
109°30'	34°24'	Weinan	Loess Plateau	650	Y	Y	Y	Y	29
110°00'	31°29'	DJH1, Dajiuhu	Shennongjia Mountains	1751	Y	Y	Y	Y	30
110°17'	21°09'	Huguangyan maar	southern China	23	Y	Y	Y	Y	31
115°57'	39°45'	East part	Yan Shan	150?	Y	Y	Y	Y	32
117°23'	20°07'	17940	S China Sea	-1727	Y			N	33
117°25'	20°03'	ODP 1144	S China Sea	-2037	Y			N	34
117°21'	20°08'	MD05-2906	S China Sea	-1636	Y	Y	Y	N	35
119°02'	26°46'	SZY peat bog	Fujian	1007	Y			Y	36
120°53'	23°49'	Toushe Basin	Taiwan	650	Y		Y	Y	37
127°16'	28°09'	DG9603	China Sea	-1100	Y			Y	38
127°22'	28°07'	MD982194	Okinawa Trough	-989	Y	Y		Y	39
118°16'	20°20'	STD235	S China Sea	-2630	Y	Y	Y	N	40



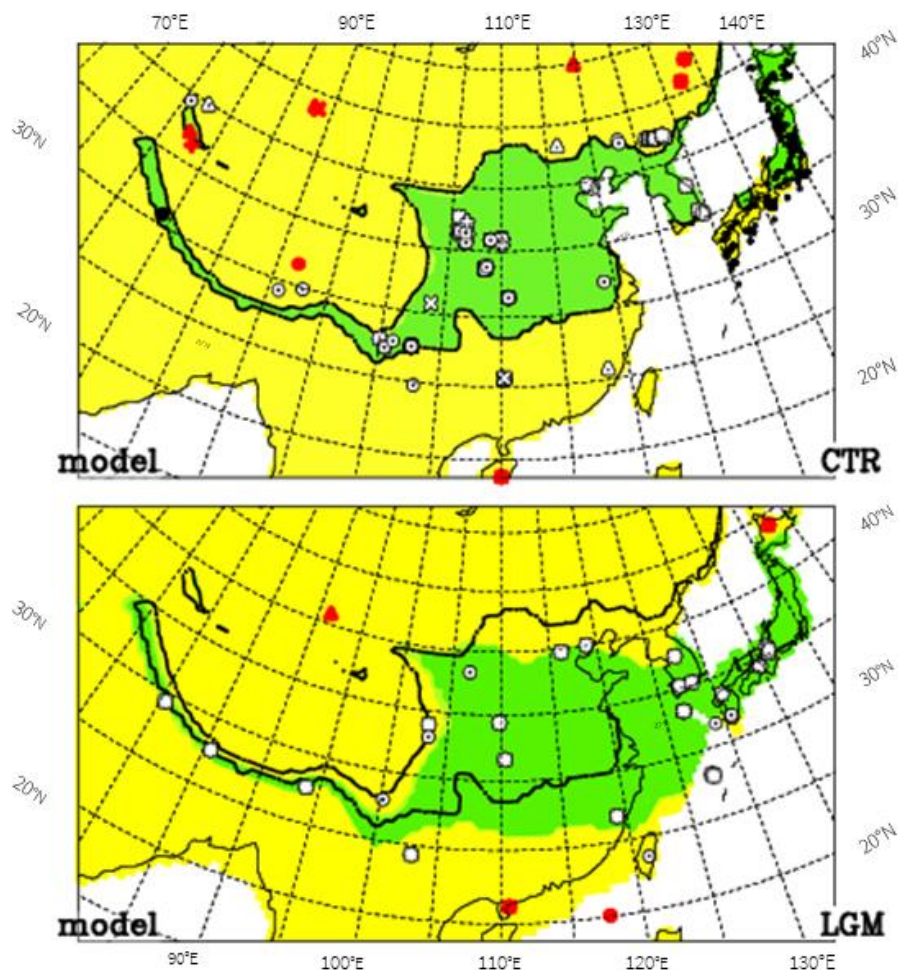
391

392 Authors: 1 Kotlia et al. 2010; 2 Fuji and Sakai 2002; 3 Bhattacharyya et al., 2014; 22 Yang et al., 2013 ; 23 Cook et al. 2011 ; 24
393 Chen et al. 2014 and Chen XM et al. 2015 IPS abstract ; 26 Shen et al. 2005 ; 27 Yan et al. 1999 ; 28 Liu Decheng et al. 2011 ;
394 29 Sun et al. 1996 ; 30 Li et al. 2013 ; 31 Wang et al., 2012, Lu et al., 2003; 32 Xu Qing-hai et al. 2002 ; 33 Sun & Li 1999;
395 Sun et al. 2000; 34 Sun et al. 2003 ; 35 Dai et al. 2015 ; 36 Yue et al. 2012 ; 37 Liew et al. 2006 ;
396 38 Xu et al. 2010 ; 39 Zheng et al. 2013 ; 40 Yu et al. 2003.

397

398 The down-scaling method used here does not allow us to present values over the emerged shelf of
399 the Yellow Sea during the LGM, when the mean sea level was 120 m below the present one
400 (Lambeck et al., 2014). Therefore in Fig. 8, the possible tree distribution is shown using model
401 data without down-scaling, when the high spatial resolution is lost and more impacts from
402 systematic errors of the model may be expected. However, fortunately, such impacts can hardly be
403 seen when comparing Fig. 6 with Fig. 8, except for the present along the southern slopes of the
404 Himalayas and the southern border of possible tree growth, where T2m by C&L is lower than that
405 of CTR (also than that by ERA), leading to a better fit with pollen data when using T2m by C&L.

406



407

408 Fig. 8: same as Fig. 6 using model data without down-scaling. The Yellow Sea is shown as land in
409 the LGM.

410

411 6 LGM CONNECTIVITY AND DISTRIBUTION MAPPING

412 The results show two worth-discussing areas with population connectivity: one is over the Yellow

413 Sea emerged shelf and one along the south of the Himalayan Range.



414 The northern limit of the temperate deciduous trees assumed by previous research (Harrison et al.,
415 2001, their figure 1) is much further south (30 - 35 °N) than what is found here. Therefore
416 population connectivity over the shelf was rejected by Harrison et al. (2001). It should be
417 mentioned that the results by Harrison et al. (2001) were based on the model available at that time
418 which had a lower resolution and also was based on observational data available at that time,
419 which have improved considerably since then. Indeed 80% of the sites used in the current
420 investigation were published post-2001. Moreover the Harrison et al. (2001) study is based on
421 biomes, not tree occurrences. Three arguments can be presented now to support this connectivity.

422 Firstly, the model results clearly show the connectivity of tree populations between China, Korea
423 and Japan during the LGM over the emerged shelf. This connectivity takes place because the limit
424 of the possible tree growth of our investigation (darker areas in Fig. 8 as well as in Fig. 6) reaches
425 still quite far north (40 °N), which is in accordance with pollen data.

426 A second argument is the presence of deciduous trees in sites located around the shelf in amounts
427 suggesting larger than simple tree presence, even perhaps woodlands or forests. In several places
428 around the emerged shelf the percentages of temperate deciduous trees indeed exceed 10%, e.g. in
429 the Yeonjaedong swamp in Korea with 20-30% of deciduous *Quercus*, 7-20 % of *Ulmus-Zelkova*
430 (Chung et al., 2010), the two sites on the Jeju island maar lake (Chung, 2007; Park and Park,
431 2015), Tenjin peatland in Japan with 12% deciduous *Quercus*, 8% *Carpinus*, 2.5% *Tilia* (Kuroda
432 and Ota, 1978), and the marine cores DG9603 and MD982194 with 15% of deciduous *Quercus*
433 (Xu et al., 2010).

434 Thirdly, information derived from recent phylogenetic investigations is supportive of the
435 occurrence of deciduous trees on the emerged shelf. For example, the phylogeography of one of
436 the most widely distributed deciduous species in eastern Asia, the oak, *Quercus variabilis*, clearly
437 suggests the occurrence of land bridges over the East China Sea (Chen et al., 2012). Around the E.
438 China Sea, other phylogenetic data indicate both mixing and absence of mixing between
439 populations depending on plant type (Qi et al., 2014). The occurrence of mixing indicates that



440 contacts were possible across the emerged shelf (e.g. Tian et al., 2016); while the absence of
441 mixing for other species indicate that not all species mixed, but certainly does not suggest total
442 absence of migration for other species. It appears therefore that the E. China Sea acted as a filter,
443 letting some through, others not (Qi et al., 2014).

444 One question, was if the pollen, found in the emerged shelf of the Yellow Sea is produced locally
445 or remotely. According to the Harrison et al. (2001) study, these pollen grains must have come
446 from the southern part of China. Yu et al. (2004) have tried to calculate such long-distance
447 transports. For *Quercus* and *Ulmus* they found transports of up to 6 ° latitude/longitude in any
448 direction. This would be too short for a transport from China south of 30 °S. Also the high pollen
449 percentages at the observed sites speak against such a long-distance transport.

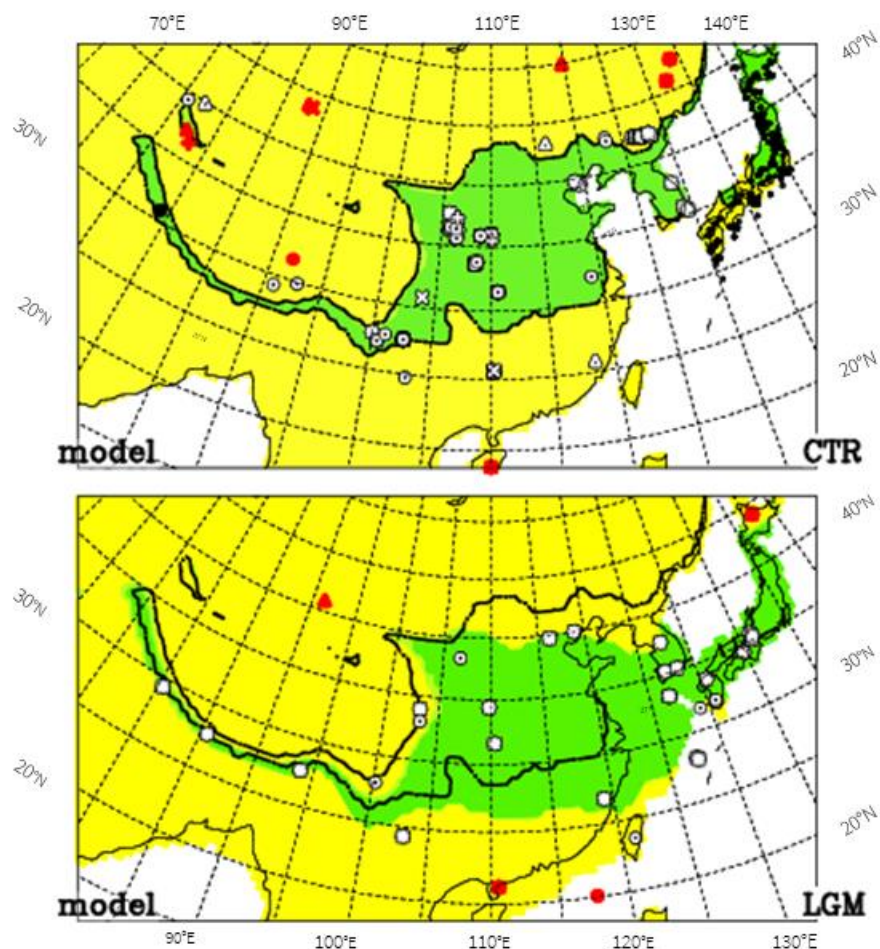
450 We are not convinced that Yu et al. (2004) calculations are robust enough for using their results in
451 our investigation, especially as their figure 3 does not agree with plant distributions by Fang et al.
452 (2009). Therefore, the wind fields for the present as analysed by ECMWF (ERA) and as simulated
453 by our model for the LGM were investigated. In Appendix S1 of Supporting Information as well as
454 in Fig. 7, it is shown that ERA and the simulation for the present agree quite well, at least for the
455 wind directions, which makes us confident that we can use the model simulations for the LGM
456 straight away.

457 The winds at 10m and 850 hPa for March, a central month for the blooming of *Quercus variabilis*,
458 are shown in Fig. 7 for the present (ERA), the CTR and the LGM. Over the emerged shelf of the
459 Yellow Sea, the 10m winds are very light from the north-west during the LGM (much stronger in
460 ERA because of the lower surface friction over the sea). For the higher level of 850 hPa, all data
461 sets show very similar distributions all with north-westerlies. Long-distance transport of deciduous
462 tree pollen would have come from NE China, an area that Harrison et al. (2001) assume to be void
463 of deciduous trees, though some recent studies (including the present one) indicate the opposite
464 (Yu et al., 2004). Further on in the year, the 850 hPa winds are blowing from the south-west,
465 starting in April (not shown) and fully crossing the 30 °N latitude in May (similar to CTR in Fig.



466 S1.1), i.e. a transport from mainland China would have been possible, though a little late for the
467 main blooming of the deciduous oak. In Appendix S1 of Supporting Information, it is shown for
468 the present that the simulations suffer from a too early progression of the monsoon front, which
469 suggests that the turn of the wind to south-westerlies may have occurred also later for the LGM,
470 thus leading to a less likely transport from mainland China.

471 The source for the pollen found in the emerged Yellow Sea is not completely clear but May is late
472 for the blooming season in central China (for Taiwan it is January to March). Therefore, a local
473 production or transport from northern China is more likely, supporting our argument that the
474 emerged Yellow Sea was occupied by deciduous trees during the LGM, as indicated by Fig. 8.



475

476 Fig. 8: same as Fig. 6 using model data without down-scaling

477 Another important population connectivity result is that the Himalayas were more favourable to

478 temperate deciduous trees in the LGM and provided the possibility of a quasi-continuous band of

479 temperate forest at its southern slope, beneficial for the spreading and diffusion of genes (e.g. for

480 Chinese mole shrew, He et al., 2016), more so than in the present (Fig. 6). Three observational

481 sites, that are currently available, support this chain of possible tree growth during the LGM. For

482 the present, this link does not exist because of too warm winter temperatures (warmer than 5 °C in

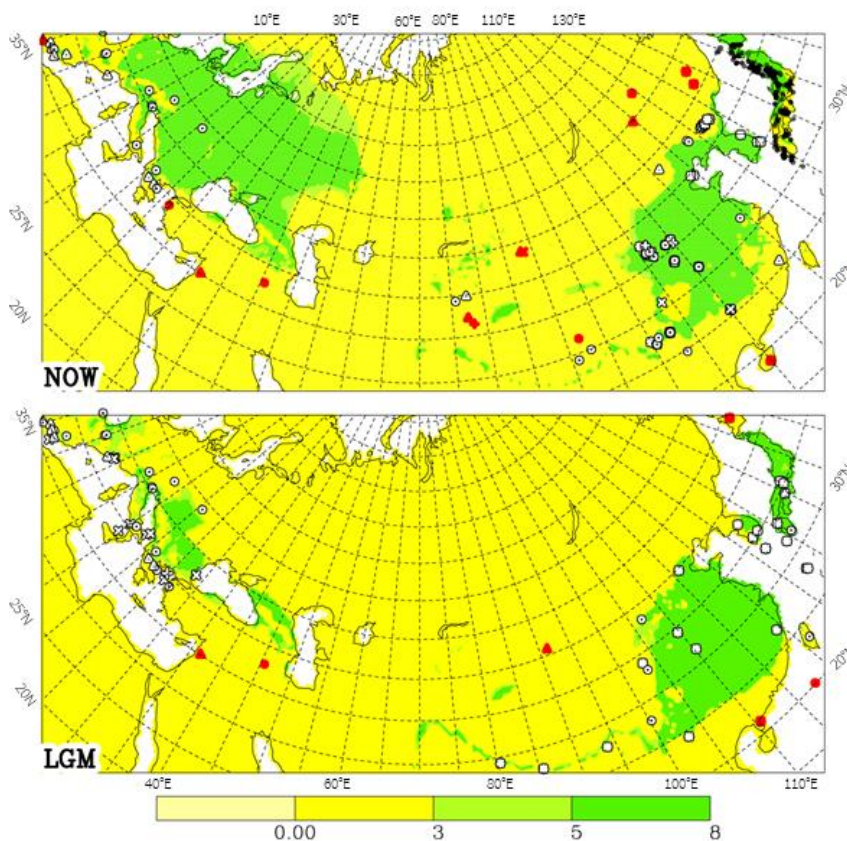


483 the C&L climatology). Along the slopes of the high Himalayas it is most likely that there would be
484 a level at which the temperature will be below 5 °C, an issue which needs further investigation).

485 Two significant cases occur where population connectivity was higher, indicating less population
486 fragmentation, in glacial than in interglacial periods. So, it appears that many tree populations live
487 nowadays in interglacial refugia.

488 Finally, this investigation shows that the model simulations suggest possible tree growth where
489 pollen grains of such trees are found. This leads to the possibility of using the model data to fill
490 gaps between observational sites by way of maps. Such gaps especially occur around 30-37 °N /
491 105-120 °E and 25-30 °N / 110-115 °E, i.e. the provinces Hupeh to Kiangsu and Hunan (ovals in
492 Fig. 6 lower panel).

493



494

495 Fig. 9: same as Fig. 6 for the whole of Eurasia.

496 By extending the view of our investigation for the whole of Eurasia (Fig. 9), a stronger link

497 between China and Europe is shown during the LGM than presently. Along the foot of the

498 Himalayas, a continuum existed; but westwards of it, still a gap north of Afghanistan (probably

499 going back to the Tertiary) is maintained, inhibiting a total link across Eurasia. This continuum is

500 broken for the present climate because winter temperatures exceed 7 °C, hence being too warm for

501 temperate deciduous trees.

502 **7 CONCLUSIONS**



503 Generally, the estimates of possible temperate deciduous tree growth in the LGM in eastern Asia
504 agree with fossil pollen observations. Therefore the model estimates can fill the areas without
505 observations. The results in the form of LGM distribution maps are considered robust enough as
506 model simulations for the present are within the range of climate estimates. Nevertheless, we are
507 aware of some uncertainties in the climate of Eastern Asia and we can safely say they are not a
508 limitation of this study.

509 During LGM the precipitation and the temperature was lower than at the present. Which of both
510 was more important for the tree growth cannot be said with certainty. Tian et al. (2016) say:
511 “annual precipitation is considered as the most important determinant”, and in our study we have
512 some indication to agree with that: In Fig. 6 and 8 there is a cluster of pollen findings over central
513 China (105-110°E/35-40°N) for the present but not for LGM. In this area the temperature does not
514 change much (Fig. 2 and 3) but the summer precipitation decreases substantially (Fig. 5). This
515 change is only slightly reflected by the boundaries of possible tree growth in Fig. 6 (north of 40°N.
516 The lack of observational sites with pollen of tree pollen is not a proof, because it could be due to
517 many reasons, but the massive change in occurrence is suggestive that we should have increased
518 summer precipitation the requirements for tree growth of summer precipitation (Table 1). This can,
519 however, also indicate the reduced water use efficiency of the trees at LGM due to lower
520 atmospheric CO₂.

521 During the LGM, major connectivities between populations are found, which is in agreement with
522 observation, i.e. less tree population fragmentation. This is especially visible in two places. Firstly,
523 the link between China, Korea and Japan is clear. Sufficient new pollen studies around and on the
524 emerged Yellow Sea shelf are now available, confirming the results of the model. They suggest the
525 presence of temperate deciduous trees, perhaps even woodlands, in the area.

526 Secondly, connectivity during the glacial period occurred at the southern slope of the Himalayan
527 chain favouring genetic flow in interglacial refugia. Currently this link does not exist because of
528 too warm winter temperatures there. Our simulations cannot be taken as a proof of this hypothesis,
529 as one cannot imagine that along the Himalayan chain there would not be a level at which the



530 winter temperatures do not exceed 5 °C also for the present day, a higher resolution data set would
531 be able to show how wide and continuous such a corridor of possible tree growth would be at the
532 present.

533 The eastern Asian case is very different from Europe, where fragmentation is the rule in the LGM.
534 In Europe (Fig. 2), the temperatures were much lower than presently (8 to 15 °C) compared to
535 Eastern Asia (3 to 5 °C) and therefore the shift of possible temperate deciduous tree growth is
536 much smaller in E. Asia than in Europe. Phylogenetic results in E. Asia are indeed in favour of the
537 hypothesis of species surviving both in the north and the south of China (Qian and Ricklefs, 2000)
538 and not of species surviving only in the south (Harrison et al., 2001). In Eastern Asia, the basic
539 expansion-contraction model of Europe was much less important (Qiu et al., 2011) due to the
540 smaller ice cap and a different topography (López-Pujol et al., 2011). Eastern Asia biodiversity
541 was therefore preserved across the Ice Ages, owing to not only the more moderate lowering of
542 temperatures but also to the better connectivity between populations.

543 Another outcome of this research is the contribution to the conservation agenda (López-Pujol et al.,
544 2001). The areas of LGM refugia often match areas of present hotspots of biodiversity. Hence the
545 distribution of temperate forest obtained in our investigation can serve as a guide to establish
546 nature parks for plants and animals. Moreover the difference between LGM and present
547 distribution contribute to the understanding of rate of distribution change (as well genetic flow),
548 which is important to monitor in light of future climatic change.

549

550 **ACKNOWLEDGMENTS**

551 Jing Zheng (Fujian Agriculture and Forestry University) started collecting the LGM data during a
552 post-doctoral stay with Suzanne Leroy at Brunel University London. Uwe Mikolajewicz
553 acknowledges funding from the German Federal Ministry of Education and Research in its
554 research framework for sustainable development (FONA3, FKZ 01LP1502A).

555

556



557 **AUTHORS CONTRIBUTION**

558 S.A.G. Leroy

559 Looking after conceptual issues, collecting the data, writing the manuscript

560

561 K. Arpe

562 Writing most of the manuscript, preparing the figures and responsible for meteorological

563 and climatological issues

564

565 U. Mikolajewicz

566 Providing the model simulations

567

568 J. Wu

569 providing observational tree pollen data

570

571

572 **The authors declare that they have no conflict of interest**

573 **Code availability**

574 The model version is already widely known and available. We have clearly described what has
575 been done and the follow up programs are written in FORTRAN This can be requested from Klaus
576 Arpe if wanted

577 **Data availability**

578 Table 2 provides a list of all observational sites and observational tree pollen data. Most of the
579 other data are referred to by giving the website. It does not seem feasible to provide the model
580 simulation data in a simple way. They can be obtained from Klaus Arpe in GRIB format.

581

582

583

584

585

586



587 **REFERENCES**

588 Annan, J. D. and Hargreaves J. C.: A new global reconstruction of temperature changes at the Last
589 Glacial Maximum. *Clim. Past*, **9**, 367–376, 2013.

590

591 Arpe K., Leroy S.A.G. and Mikolajewicz U.: A comparison of climate simulations for the last
592 glacial maximum with three different versions of the ECHAM model and implications for
593 summer-green tree refugia. *Clim. Past*, **7**, 1–24, 2011.

594

595 Becker A, Finger P, Meyer-Christoffer A, Rudolf B, Schamm K, Schneider U, Ziese M : A
596 description of the global land-surface precipitation data products of the Global Precipitation
597 Climatology Centre with sample applications including centennial (trend) analysis from 1901
598 present. *Earth Syst. Sci. Data* 5: 71-99, DOI: 10.5194/essd-5-71-2013, 2013.

599

600 Bhattacharyya A., Mehrotra N., Shah S. K., Basavaiah N., Chaudhary V., Singh IB, and Singh
601 I.B.: Analysis of vegetation and climate change during Late Pleistocene from Ziro Valley,
602 Arunachal Pradesh, Eastern Himalaya region. *Quatern Sci Rev* 101, 111-123, 2014.

603

604 Braconnot P., B. Otto-Bliesner, Harrison S., Joussaume S., Peterchmitt J-Y. Abe-Ouchi M.,
605 Crucifix M., Driesschaert E, Fichefet Th., Hewitt C. D., Kageyama M., Kitoh A., **Lainé A.**,
606 Loutre M.-F., Marti O., Merkel U., Ramstein G., Valdes P., Weber S. L., Yu Y., and Zhao Y.
607 : Results of PMIP2 coupled simulations of the Mid-Holocene and Last Glacial Maximum – Part
608 1: experiments and large-scale features. *Clim. Past*, **3**, 261–277, 2007.

609

610 Cao, X., Ni, J., Herzschuh, U., Wang, Y. and Zhao Y.: A late Quaternary pollen dataset from
611 eastern continental Asia for vegetation and climate reconstructions: Set up and evaluation.
612 *Palaeobot Palyno* 194, 21–37, 2013.

613



- 614 Chen D., Zhang X., Kang H., Sun X., Yin S., Du H., Yamanaka N., Gapare W., Wu H. X. and Li
615 C. : Phylogeography of *Quercus variabilis* Based on Chloroplast DNA Sequence in East Asia:
616 Multiple Glacial Refugia and Mainland-Migrated Island Populations. PloS One, 7,10: e47268.
617 doi:10.1371/journal.pone.0047268, 2012.
- 618
- 619 Chen W.-Y., Su T., Adams J.M., Jacques F.M.B., Ferguson D.K. and Zhou Z.-K: Large-scale
620 dataset from China gives new insights into leaf margin–temperature relationships. Palaeogeogr,
621 Palaeocl 402, 73–80, 2014.
- 622 Chen J., Liu Y., Shi X., Bong-Chool S., Zou J. and Yao Z.: Climate and environmental changes for
623 the past 44 ka clarified in the Ulleung Basin, East Sea (Japan Sea). Quat Int, 1-12, 2016,
624
- 625 Chen X.M., Chen F., Zhou A., Wu D., Chen J. and Huang X.: Vegetation history, climatic changes
626 and Indian summer monsoon evolution during the last 36400 years documented from sediments
627 of Xingyun Lake, south-west China. 13th International Paleolimnological Symposium,
628 Lanzhou, China, volume of abstracts, pages 162-163, 2015.
- 629
- 630 Chung C.-H, Lim HS and Yoon HI: Vegetation and climate changes during the Late Pleistocene to
631 Holocene inferred from pollen record in Jinju area, South Korea. Geosci J 10, 4, 423 – 431,
632 2006.
- 633
- 634 Chung C.-H. : Vegetation response to climate change on Jeju Island, South Korea, during the last
635 deglaciation based on pollen record. Geosci J 11, 2, 147 – 155, 2007.
- 636 Chung C.-H., Lim H. S. and Lee H. J.: Vegetation and climate history during the late Pleistocene
637 and early Holocene inferred from pollen record in Gwangju area, South Korea. Quatern Int 227,
638 61-67, 2010.
- 639



- 640 CLIMAP: Seasonal reconstructions of the Earth's surface at the last glacial maximum,
641 Geological Society of America, Map Chart Ser., MC-36, 1981.
642
- 643 Cook C. G., Jones R. T., Langdon P. G., Leng M.G. and Zhang E: New insights on Late
644 Quaternary Asian palaeomonsoon variability and the timing of the Last Glacial Maximum in
645 southwestern China.. *Quatern Sci Rev* 30, 808-820, 2011
646
- 647 Cramer W. : www.pik-potsdam.de/~cramer/climate.html, last accessed 2007, 1996.
648
- 649 CRU: www.cru.uea.ac.uk/cru/data/hrg last accessed January 2016.
650
- 651 Dai L., Weng C. and Limi M: Patterns of vegetation and climate change in the South China Sea
652 during the last glaciation inferred from marine palynological records. *Paleogeography,*
653 *Paleoclimatology, Paleoecology*, 440, 249-258, 2015.
- 654 Dee D. P., Uppala S. M., Simmons A. J., Berrisford P., Poli P., Kobayashi S., Andrae U.,
655 Balmaseda M. A., Balsamo G., Bauer P., Bechtold P., Beljaars A. C. M., van de Berg L., Bidlot
656 J., Bormann N., Delsol C., Dragani R., Fuentes M., Geer A. J., Haimberger L., Healy S. B.,
657 Hersbach H., Hólm E.V., Isaksen L., Kállberg P., Köhler M., Matricardi M., McNally A. P.,
658 Monge-Sanz B. M., Morcrette J.-J., Park B.-K., Peubey C., de Rosnay P., Tavolato C., Thépaut
659 J.-N. and Vitart F: The ERA -Interim reanalysis: configuration and performance of the data
660 assimilation system. *Q J Ro Meteor Soc* 137(656): 553–597, Part A. doi: 10.1002/qj.828,
661 2011.
662
- 663 Donoghue M. J. and Smith S. A.: Patterns in the assembly of temperate forests around the Northern
664 Hemisphere. *Phil. Trans. R. Soc. Lond. B* 359, 1633–1644, 2004.
665



666 ECMWF: http://data-portal.ecmwf.int/data/d/interim_daily/. Last accessed May 2014. Present
667 address: <https://apps.ecmwf.int/datasets/data/interim-full-mnth/levtype=sfc/>
668 Fang J, Wang Z and Tang Z: Atlas of woody plants in China. Higher Education Press, Beijing, pp
669 2020, 2009
670
671 Fuji R. and Sakai H. : Paleoclimatic changes during the last 2.5 myr recorded in the Kathmandu
672 Basin, central Nepal Himalayas. J of Asian Earth Sci 20: 255-266, 2002.
673
674 Gotanda K., Nakagawa T., Tarasov P., Kitagawa J., Inoue Y. and Yasuda Y.: Biome classification
675 from Japanese pollen data: application to modern-day and Late Quaternary samples. Quatern
676 Sci Rev 21, 647–657, 2002.
677
678 Gotanda K. and Yasuda Y. :Spatial biome changes in southwestern Japan since the Last Glacial
679 Maximum. Quatern Int 184, 84–93, 2008.
680
681 GPCC: ftp://ftp-anon.dwd.de/pub/data/gpcc/html/download_gate.html. Last accessed January 2014,
682 2013.
683
684 Harrison S. P., Yu G., Takahara H. and Prentice I. C. : Diversity of temperate plants in east Asia.
685 *Nature* 413, 129-130, 2001.
686
687 Hayashi R., Takahara H., Hayashida A. and Takemura K.: Millennial-scale vegetation changes
688 during the last 40,000 yr based on a pollen record from Lake Biwa, Japan. Quaternary Res. 74,
689 91-99, 2010.
690



- 691 He K., Hu N.-Q., Chen X., Li J.-T. and Jiang X.-L. : Interglacial refugia preserved high genetic
692 diversity of the Chinese mole shrew in the mountains of southwest China. *Heredity* 116: 23-32.
693 2016.
- 694 Igarachi Y.: Pollen record in core MD01-2421 off Kashima, North Pacific: correlation with the
695 terrestrial pollen record since MIS 6. *Jour. Geol. Soc. Japan*, 115,7, 357-366, 2009.
- 696 Igarachi Y. and Zharov A. E.: Climate and vegetation change during the late Pleistocene and early
697 Holocene in Sakhalin and Hokkaido, northeast Asia. *Quatern Int* 237, 24-31, 2011.
- 698
- 699 Jiang D. and Lang X.: Last Glacial Maximum East Asian Monsoon: Results of PMIP Simulations.
700 *Jour. of Clim*, 23, 5030 - 5038. DOI: 10.1175/2010JCLI3526.1, 2010.
- 701
- 702 Kawahata H. and Ohshima H: Vegetation and environmental record in the northern East China Sea
703 during the late Pleistocene. *Global Plane Change* 41,251–273, 2004.
- 704
- 705 Kim S.-J., Crowley T. J., Erickson D. J., Govindasamy B., Duffy P. B. and Lee B. Y.: High-
706 resolution climate simulation of the last glacial maximum. *Clim Dyn* 31:1–16 DOI
707 10.1007/s00382-007-0332-z, 2008.
- 708
- 709 Kotlia B. S., Sanwal J., Phartiyal B., Joshi L., Trivedi A. and Sharma C.: Late Quaternary climatic
710 changes in the eastern Kumaun Himalaya, India, as deduced from multi-proxy studies. *Quatern*
711 *Int* 213, 44–55, 2010.
- 712 Kucera, M., Weinelt, M., Kiefer, T., Pflaumann, U., Hayes, A., Chen, M. T., Mix, A. C., Barrows,
713 T. T., Cortijo, E., Duprat, J., Juggins, S., and Waelbroeck, C.: Reconstruction of Sea-Surface
714 Temperatures from Assemblages of Planktonic Foraminifera: Multi-Technique Approach Based
715 on Geographically Constrained Calibration Data Sets and Its Application to Glacial Atlantic and
716 Pacific Oceans, *Quaternary Sci. Rev.*, 24, 951–998, 2005.
- 717



- 718 Kumon F, Kawai S. and Inouchi Y.: Climate Changes between 25000 and 6000 yrs BP Deduced
719 from TOC, TN, and Fossil Pollen Analyses of a Sediment Core from Lake Nojiri, Central
720 Japan. *The Quaternary Res* 42, 1: 13-26, 2003.
- 721 Kuroda T. and Ota T.: Palynological study of the late Pleistocene and Holocene deposits of the
722 Tenjin area, Fukuoka City, northern Kyushu, part 1. *The Quaternary Res* 17, 1, 1-14. (In
723 Japanese with English summary), 1978.
- 724
- 725 Lambeck K., Rouby H., Purcell A., Sun Y., and Sambridge M.: Sea level and global ice volumes
726 from the Last Glacial Maximum to the Holocene. *PNAS* 111, 43, 15296–15303, 2014.
- 727
- 728 Leemans R. and Cramer W.: The IIASA database for mean monthly values of temperature,
729 precipitation and cloudiness of a global terrestrial grid, International Institute (IIASA). RR-91-
730 18, 1991.
- 731
- 732 Leroy S. A. G.: Progress in palynology of the Gelasian-Calabrian Stages in Europe: ten messages,
733 *Revue de Micropaléontologie*, 50, 293–308, 2007.
- 734
- 735 Leroy S. and Arpe K.: Glacial refugia for summer-green trees in Europe and S-W Asia as proposed
736 by ECHAM3 time slice atmospheric model simulations. *J Biogeogr*, 34, 2115-2128. doi:
737 10.1111/j.1365-2699.2007.01754x, 2007.
- 738 Li J. and Del Tredici P.: The Chinese *Parrotia*: A Sibling Species of the Persian *Parrotia*. *Arnoldia*
739 66,1: 2-9, 2008.
- 740
- 741 Li J., Zheng Z., Huang K., Yang S., Chase B., Valsecchi V., Carré M. and Cheddadi R.: Vegetation
742 changes during the past 40,000 years in Central China from a long fossil record. *Quatern Int*
743 310, 221-226, 2013.

744 .



- 745 Liao J. C.: Fagaceae. In *Flora of Taiwan*. Volume 2. 2nd edition. Edited by: Boufford D. E., Hsieh
746 C. F., Huang T. C. , Ohashi H., Yang Y. P and Lu S. Y.. Taipei, Taiwan: Editorial Committee of
747 *Flora of Taiwan*; 114–115, 122, 1996.
748
- 749 Liew P.-M., Huang S.-Y. and Kuo C.-M.: Pollen stratigraphy, vegetation and environment of the
750 last glacial and Holocene—A record from Toushe Basin, central Taiwan. *Quatern Int* 147, 16–
751 33, 2006.
752
- 753 Liu D., Gao X., Wang X., Zhang S., Pei S. and Chen F.: Palaeoenvironmental changes from
754 sporopollen record during the later Late Pleistocene at Shuidonggou locality 2 in Yinchuan,
755 Ningxia. *Journal of Palaeogeography*, 13, 4, 467-472 (in Chinese with English abstract), 2011.
756
- 757 López-Pujol J., Zhang F.-M., Sun H.-Q., Ying T.-S. and Ge S.: Mountains of southern China as
758 “Plant Museums” and “Plant Cradles”: evolutionary and conservation insights. *Mountain*
759 *Research and Development* 31, 3: 261-269, 2011.
760
- 761 Lu H.-Y., Liu J.-Q., Chu G.-Q., Gu Z.-Y., Negendank J., Schettler G. and Mingram J.: A study of
762 pollen and environment in the Huguangyan maar lake since the last glaciation. *Acta*
763 *Palaeontologica Sinica* 42, 2, 284-291, 2003.
764
- 765 Mikolajewicz, U., Vizcaino, M., Jungclaus, J., and Schurgers, G.: Effect of ice sheet interactions in
766 anthropogenic climate change simulations, *Geophys. Res. Lett.*, 34, L18706,
767 doi:10.1029/2007GL031173, 2007.
768
- 769 Milne R. I. and Abbott R. J.: The Origin and Evolution of Tertiary Relict Floras. *Advances in*
770 *Botanical Research* Vol. 38: 281-314, 2002.
771



- 772 Mix A. C., Bard E. and Schneider, R.: Environmental processes of the ice age: land, oceans,
773 glaciers (EPILOG), *Quaternary Sci. Rev.*, 20, 627–657, 2001.
- 774
- 775 Molavi-Arabshahi M., Arpe K. and Leroy S. A. G.: Precipitation and temperature of the south-
776 west Caspian Sea region during the last 55 years, their trends and teleconnections with large-
777 scale atmospheric phenomena. *International Journal of Climatology*. DOI: 10.1002/joc.4483,
778 2015.
- 779
- 780 Momohara A., Yoshida A., Kudo Y. and Nishiuchi, Okitsu S.: Paleovegetation and climatic
781 conditions in a refugium of temperate plants in central Japan in the Last Glacial Maximum.
782 *Quatern Int* 425, 38-48, 2016.
- 783
- 784 Miyoshi N. and Yano N.: Late Pleistocene and Holocene vegetation history of Ohnuma moor in
785 the Chugoku Mountains, western Japan. **Rev Palaeobot Palyno**
786 46, 355-376, 1986.
- 787
- 788 Nakagawa T., Tarasov P.E., Nishida K., Gotanda K. and Yasuda Y.: Quantitative pollen-based
789 climate reconstruction in central Japan: application to surface and Late Quaternary spectra.
790 *Quaternary Science Reviews* 21, 2099–2113, 2002.
- 791
- 792 Ni J., Yu G., Harrison S.P. and Prentice I.C.: Palaeovegetation in China during the late Quaternary:
793 biome reconstructions based on a global scheme of plant functional types. *Palaeogeogr.*
794 *Palaeoclimatol. Palaeoecol.* 289, 44–61, 2010.
- 795
- 796 Ni J., Cao X., Jeltsch F. and Herzschuh U.: Biome distribution over the last 22,000 yr in China.
797 *Palaeogeogr. Palaeoclimatol.* 409, 33–47, 2014.



- 798 Nishiuchi R., Momohara A., Osato S. and Endo K: Temperate deciduous broadleaf forest dynamics
799 around the last glacial maximum in a hilly area in the northern Kanto district, central Japan.
800 Quatern Int 455: 113-125, 2017.
801
- 802 Orain R., Lebreton V., Russo Ermolli E., Combourieu-Nebout N. and Sémah A.-M.: *Carya* as
803 marker for tree refuges in southern Italy (Boiano basin) at the Middle Pleistocene. Palaeogeogr,
804 Palaeocl 369, 295–302, 2013.
805
- 806 Park J.: A modern pollen–temperature calibration data set from Korea and quantitative temperature
807 reconstructions for the Holocene. The Holocene, 21 (7) 1125–1135, 2011.
808
- 809 Park J. and Park J.: Pollen-based temperature reconstructions from Jeju island, South Korea and its
810 implication for coastal climate of East Asia during the late Pleistocene and early Holocene.
811 Palaeogeogr, Palaeocl 417, 445–457, 2015.
812
- 813 Piggott D.: Lime-trees and Basswoods: A Biological Monograph of the Genus *Tilia*. 395pp.
814 Cambridge University Press, Cambridge, UK, 2012.
815
- 816 Qi XS, Yuan N, Comes HP, Sakaguchi S, and Qiu YX: A strong ‘filter’ effect of the East China
817 Sea land bridge for East Asia’s temperate plant species: inferences from molecular
818 phylogeography and ecological niche modelling of *Platycrater arguta* (Hydrangeaceae). BMC
819 Evolutionary Biology, 14:41, 2014.
820
- 821 Qian H. and Ricklefs RE: Large-scale processes and the Asian bias in species diversity of
822 temperate plants. Nature 407: 180-182, 2000.
823



- 824 Qiu Y.X., Fu C.X. and Comes HP.: Plant molecular phylogeography in China and adjacent
825 regions: Tracing the genetic imprints of Quaternary climate and environmental change in the
826 world's most diverse temperate flora. *Molecular Phylogenetics and Evolution* 59, 225–244,
827 2011.
- 828
- 829 Reichler, T., and J. Kim: How Well do Coupled Models Simulate Today's Climate?
830 *Bull. Amer. Meteor. Soc.*, 89, 303-311, 2008.
- 831
- 832 Roche D. M., Dokken T. M., Goosse H., Renssen H., and Weber S. L.: Climate of the last glacial
833 maximum: sensitivity studies and model-data comparison with the LOVECLIM coupled model.
834 *Clim. Past*, 3, 205-224, 2007.
- 835
- 836 Roeckner, E., B'auuml, G., Bonaventura, L., Brokopf, R., Esch, M., Giorgetta, M., Hagemann, S.,
837 Kirchner, I., Kornblueh, L., Manzini, E., Rhodin, A., Schlese, U., Schulzweida, U., and
838 Tompkins, A.: The atmospheric general circulation model ECHAM5, Part I: Model description,
839 Max Planck Institute for Meteorology, Hamburg, Report no. 349, 2003.
- 840
- 841 Schneider U., Becker A., Finger P., Meyer-Christoffer A., Rudolf B. and Ziese M.: GPCC Full
842 Data Reanalysis Version 6.0 at 0.5: Monthly Land-Surface Precipitation from Rain-Gauges
843 built on GTS-based and Historic Data. DOI: 10.5676/DWD_GPCC/FD_M_V6_050, 2011.
- 844
- 845 Shen C., Tang L., Wang S., Li C. and Liu K.: The Pollen Records and time scale from the RM of
846 the Zoige Basin, northeastern Qinghai-Tibetan Plateau. *Chinese Science Bulletin*, 50, 6, 553-
847 562, 2005.
- 848



- 849 Sitch S., Smith B., Prentice I. C., Arneth A., Bondeau A., Cramer W., Kaplan J.O., Levis S., Lucht
850 W., Sykes M. T., Thonicke K. and Venevsky S.: Evaluation of ecosystem dynamics, plant
851 geography and terrestrial carbon cycling in the LPJ Dynamic Global Vegetation Model. *Global*
852 *Change Biology* 9, 161-185, 2003.
- 853
- 854 Shimada M., Takahara H., Imura R., Haraguchi T., Yonenobu H. I. Hayashida A. and Yamada K.:
855 Vegetation history based on pollen and charcoal analyses since the Last Glacial Maximum in
856 southern Kyushu, Japan. EPPC Padua Italy 26-21 August 2014, abstract book p. 253, 2014.
- 857
- 858 Solla A., Martin JA and Corral P, Gil L.: Seasonal changes in wood formation of *Ulmus pumila*
859 and *U. minor* and its relation with Dutch elm disease. *New Phytologist* 166, 1025-1034, 2005.
- 860
- 861 Sugaya M., Okuda M. and Okada M.: Quantitative paleoclimate reconstruction based on a 130 ka
862 pollen record from teC9001C core off NE Japan. *Quatern Int* 397, 404-416, 2016.
- 863
- 864 Sun X. J., Song C. Q. and Wang F. Y.: Vegetation history of the Southern Loess Plateau of China
865 during the last 100,000 years based on pollen data. *Acta Botanica Sinica*, 38, 12, 982-988. (in
866 Chinese with English summary), 1996.
- 867
- 868 Sun X.J. and Li X.: A pollen record of the last 37 ka in deep sea core 17940 from the northern
869 slope of the South China Sea. *Marine Geology*, 156, 227-244. 1999.
- 870
- 871 Sun X., Li X., Luo Y. and Chen X.: The vegetation and climate at the last glaciation on the
872 emerged continental shelf of the South China Sea. *Palaeogeogr. Palaeocl* 160, 301-316, 2000.
- 873



- 874 Sun X., Luo Y, Huang F., Tian J. and Wang P.: Deep-sea pollen from the South China Sea:
875 Pleistocene indicators of East Asian monsoon. *Marine Geology* 201, 97-118, 2003.
876
- 877 Svenning J.-C.: Deterministic Plio-Pleistocene extinctions in the European cool-temperate tree
878 flora. *Ecology Letters*, 6: 646–653, 2003.
879
- 880 Takahara H. and Takeoka M.: Vegetational changes since the last Glacial maximum around the
881 Hatchodaira Moor, Kyoto, Japan. *Japan Journal Ecology* 36, 105-116, 1986.
882
- 883 Takahara H. and Takeoka M.: Vegetation history since the last glacial period in the Mikata
884 lowland, the Sea of Japan area, western Japan. *Ecological Research* 7, 371-386, 1992.
- 885 Takahara Hi, Sugita S., Harrison S.P., Miyoshi N., Morita Y. and Uchiyama T.: Pollen-based
886 reconstructions of Japanese biomes at 0, 6000 and 18,000 14C yr BP. *J Biogeogr*, 27, 665–683,
887 2000.
888
- 889 Tian B, Liu R., Wang L., Qiu Q., Chen K. and Liu J.: Phylogeographic analyses suggest that a
890 deciduous species (*Ostryopsis davidiana* Decne., Betulaceae) survived in northern China during
891 the Last Glacial Maximum. *J Biogeogr* 36, 2148–2155., 2009.
892
- 893 Tian F., Cao X., Dallmeyer A., Ni J., Zhao Y., Wang Y. and Herzschuh U.: Quantitative woody
894 cover reconstructions from eastern continental Asia of the last 22 kyr reveal strong regional
895 peculiarities. *Quatern Sci Rev*, 137, 33-44, 2016.
896
- 897 Tian Z. and Jiang D.: Revisiting last glacial maximum climate over China and east Asian monsoon
898 using PMIP3 simulations. *Palaeogeogr, Palaeoclimatol, 453, 115-126, 2016.*
899



- 900 Wang S., Lu H., Han J., Chu G., Liu J. and Negendank J. F. W.: Palaeovegetation and
901 palaeoclimate in low-latitude southern China during the Last Glacial Maximum. *Quatern Int*
902 248, 79-85, 2012.
- 903
- 904 Willis KJ. and Niklas KJ.: The role of Quaternary environmental change in plant macroevolution:
905 the exception or the rule? *Phil. Trans. R. Soc. Lond. B* 359, 159–172. 2004.
- 906
- 907 Wu G., Qin J., Deng B. and Li C.: Palynomorphs in the first paleosol layer in the Yangtze Delta
908 and their paleoenvironmental implication. *Chinese Science Bulletin*. 47, 21, 1837-1842, 2002.
- 909
- 910 Xu D., Lu H, Wu N and Liu Z.: 30 000-Year vegetation and climate change around the East China
911 Sea shelf inferred from a high-resolution pollen record. *Quatern Int* 227, 53-60, 2010.
- 912
- 913 Xu G., Yang X., Ke Z., Li Nag W. and Yang Z.: Environment Changes in Yanshan Mountain
914 Area during the Latest Pleistocene. *Geography and Territorial Research*, 18, 2, 4 pages, 2002.
- 915
- 916 Yan G., Wang F.B., Shi G.R. and Li S.F.: Palynological and stable isotopic study of
917 palaeoenvironmental changes on the northeastern Tibetan plateau in the last 30,000 years.
918 *Palaeogeogr, Palaeocl* 153, 147–159, 1999.
- 919
- 920 Yang D., Peng Z., Luo C., Liu Y., Zhang Z., Liu W. and Zhang P.: High-resolution pollen
921 sequence from Lop Nur, Xinjiang, China: Implications on environmental changes during the
922 late Pleistocene to the early Holocene. ***Palaeobot Palyno*** 192, 32–41, 2013.
- 923
- 924 Yi S. and Kim S.-J.: Vegetation changes in western central region of Korean Peninsula during the
925 last glacial (ca. 21.1–26.1 cal kyr BP). *Geosci J* 14, 1, 1 – 10, 2010.
- 926



- 927 Yu S, Zheng Z., Chen Z, Jing X, Kershaw P., Moss P., Peng X., Zhang X., Chen C., Zhou Y.,
928 Huang K. and Gan H.: A last glacial and deglacial pollen record from the northern South China
929 Sea: New insight into coastal-shelf paleoenvironment. *Quatern Sci Rev* 157, 114-128, 2017.
930
- 931 Yu G., Ke X., Xue B. and Ni J.: The relationships between the surface arboreal pollen and the
932 plants of the vegetation in China. *Palaeobot Palyno* 129, 187– 198, 2004.
933
- 934 Yue Y., Zheng Z., Huang K., Chevalier M., Chase B. M., Carré M., Ledru M.-P. and Cheddadi R.:
935 A continuous record of vegetation and climate change over the past 50,000 years in the Fujian
936 Province of eastern subtropical China. *Palaeogeogr, Palaeocl* 365–366:115–123, DOI:
937 10.1016/j.palaeo.2012.09.018, 2012.
938
- 939 Zheng Z., Huang K., Deng Y., Cao L., Yu S., and Suc J.-P.: A 200 ka pollen record from Okinawa
940 Trough: Paleoenvironment reconstruction of glacial-interglacial cycles. *Science China Earth*
941 *Sciences* 56 (10), 1731-1747, 2013.
942
- 943 Zheng Z., Wei J., Huang K., Xu Q., Lu H., Tarasov P., Luo C., Beaudouin C., Deng Y., Pan A.,
944 Zheng Y., Luo Y., Nakagawa T., Li C., Yang S., Peng H. and Cheddadi R.: East Asian pollen
945 database: modern pollen distribution and its quantitative relationship with vegetation and
946 climate. *J Biogeogr.* doi:10.1111/jbi.12361, 2014.
947
- 948 Ziska, L. H. and Caulfield, F. A.: Rising CO₂ and pollen production of common ragweed
949 (*Ambrosia artemisiifolia*), a known allergy inducing species: implications for public health,
950 *Aust. J. Plant Physiol.*, 27, 893–898, 2000,
951
952



953 **BIOSKETCH**

954 Suzanne Leroy is a physical geographer, specialised in palynology. She works at various time scales and
955 resolutions from the Pliocene to the present in the Mediterranean basin, NW Africa and SW Asia as well as
956 further to the east (Kyrgyzstan and NE China), always in a multidisciplinary way, mostly in cooperation with
957 geologists and archaeologists for understanding past environments and climates, the origin of sediments, and
958 the interactions between nature and humans. Although the analysed sediments were mostly lacustrine,
959 additional experiences are in marine and deltaic environments. Recently she developed an interest in
960 phylogeography and environmental catastrophes.

961 Author contributions: S.L. is responsible for the overall research and collected the pollen data with help by
962 J.W., K.A. is responsible for the meteorology and climatology aspects as well as did most of the
963 programming and writing of the manuscript, U.M. provided the climate model simulations and J.W.
964 contributed to the data search and typical Chinese aspects.

965